CHIN. PHYS. LETT. Vol. 32, No. 2 (2015) 020703

Label-Free and Real-Time Monitor of Binding and Dissociation Processes between Protein A and Swine IgG by Oblique-Incidence Reflectivity Difference Method *

HE Li-Ping(何立平)[1], LIU Shuang(刘爽)[1], DAI Jun(戴俊)[1], WU Lin(吴琳)[2], LIU Guo-Zhen(刘国振)[3], WEI Han-Fu(韦汉福)[3], LU Hui-Bin(吕惠宾)[1]**, JIN Kui-Juan(金奎娟)[1], YANG Guo-Zhen(杨国桢)[1]

[1]*Beijing National Laboratory for Condensed Matter Physics, Institute of Physics, Chinese Academy of Sciences, Beijing 100190*

[2]*Key Laboratory of Genome Sciences and Information, Beijing Institute of Genomics, Chinese Academy of Sciences, Beijing 100101*

[3]*Beijing Protein Innovation Co. Ltd., Beijing 101318*

(Received 29 September 2014)

Life science has a need for detection methods that are label-free and real-time. In this paper, we have selected staphylococcal protein A (SPA) and swine immunoglobulin G (IgG), and monitor the bindings between SPA and swine IgG with different concentrations, as well as the dissociations of SPA-swine IgG complex in different pH values of phosphate buffer by oblique-incidence reflectivity difference (OIRD) in a label-free and real-time fashion. We obtain the ON and OFF reaction dynamic curves corresponding to the bindings and dissociations of SPA and swine IgG. Through our analysis of the experimental results, we have been able to obtain the damping coefficients and the dissociation time of SPA and swine IgG for different pH values of the phosphate buffer. The results prove that the OIRD technique is a competing method for monitoring the dynamic processes of biomolecule interaction and achieving the quantitative information of reaction kinetics.

PACS: 07.60.Fs, 81.70.Fy, 87.80.Dj, 83.85.Ei DOI: 10.1088/0256-307X/32/2/020703

Interactions between numerous biomolecules are crucial if they are to carry out biological functions. However, it has always been challenging for the life sciences to obtain a detection method that is label-free and has a high-throughput. Up until to now, most detection methods have been label-based,[1,2] in which the extrinsic label would probably impact the biomolecular characteristics and the natural activities.[3,4] In addition, label-dependent detection methods are mostly used for end-point detection and are not amenable to monitor the dynamic process of biomolecular interactions.[3,4] Although some label-free detection methods, such as surface plasmon resonance (SPR),[5,6] have shown an ability to monitor biomolecular interactions in real time, the SPR is limited to be only used in some fields due to the fact that SPR needs a valuable slide that is coated with gold, in addition to which the throughput is not high enough.

Oblique-incidence reflectivity difference (OIRD) is a label-free high-throughput and real-time method for detecting the interactions of biomolecules.[7−10] As mentioned in our previous studies,[9,10] the OIRD method measures the fractional difference between the reflectivity of the p- and s-polarized lights from a surface under the condition of oblique incidence, i.e., $\Delta_{\rm p} - \Delta_{\rm s}$. We have reported the use of the OIRD method to determine the kinetics of antigen-antibody interactions,[10−13] oligonucleotides hybridization,[14] dynamic processes of protein degradation,[15] protein-DNA interactions,[16] DNA hybridization,[17] and protein-protein interactions.[18,19] This method has been proven to be highly reproducible.[20] In this Letter, we further explore the ability of the OIRD method to monitor the binding and dissociation processes of biomolecules by studying the binding and dissociation feature between staphylococcal protein A (SPA) and swine immunoglobulin G (IgG).

SPA is a surface protein that is originally found in the cell wall of the bacteria staphylococcus aureus. SPA is able to bind IgG, thus it is commonly used in biochemical research for IgG purification,[21] immunoprecipitation (pulling down of protein complexes through target-specific antibodies), and so on. In these applications, SPA is normally immobilized onto a solid support, such as agarose beads, for the ease of washing away non-interacted components and finally collecting samples dissociated from SPA. The dissociation feature of SPA and IgG depends on the pH value of ambience.[22] Generally, IgG binds SPA in neutral ambience and dissociates in a new ambience with an acidic pH value mostly around 4.0. The refined IgG solution is then rapidly neutralized due to the fact that exposure to extreme pH may damage its activity. Study of its dynamic dissociation feature will help to select the optimal pH value under the best purification condition in which IgG activity damage is minimized and its production is maximized.

*Supported by the Key Research Program of Chinese Academy of Sciences.

**Corresponding author. Email: hblu@iphy.ac.cn

In this work we have monitored the both bindings between SPA and swine IgG with different concentrations and their dissociations in solutions with different pH values by OIRD in a label-free and real-time fashion. To monitor the entire processes in parallel, five identical fluid cavities were designed based on our previous OIRD device. Every cavity connects individually with one fluid channel, such that the biomolecule interactions in every cavity are independent.

As shown in Fig. 1, we fabricated the SPA microarrays, including five identical line arrays (marked 1, 2, 3, 4, and 5), using a conventional printing procedure. Each line array includes four duplicated SPA spots and four duplicated Bovine Serum Albumin (BSA) spots as a control. The five line arrays are arranged in a line and positioned in such a way that each fluid cavity contains one line array. The red dashed line with arrows indicates the scanning path of the detection light spot of the OIRD.

To fabricate the SPA microarrays, SPA (Bino Biological Inc.) of 1.0 mg/mL and BSA of 1.0 mg/mL in 1 × phosphate buffered saline (PBS) solution were printed on the epoxy group-functionalized glass slides by a contact printing robot. The resulting SPA and BSA sample spots are circular with an average diameter of ∼100 μm and a center-to-center distance of 300 μm. The prepared SPA microarrays were at 4℃ for 12 h for SPA and BSA molecules to better covalently attach on the epoxy surface. Then, the microarrays were washed by stirring with double distilled water (ddH_2O) for 5 min to wash away free SPA and BSA molecules. After that, the microarray was mounted on the scanning platform of the OIRD device and the five line arrays in the microarray were sealed in the five fluid cavities individually. The microarray was blocked for 20 min with 0.25 mg/mL BSA solution to quench any exposed free epoxy groups on the microarray surface. Therewith, the BSA solution was drained and the five cavities were filled with ddH_2O.

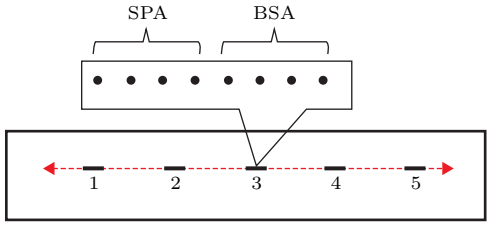

Fig. 1. The layout of the SPR microarray which contains five identical line arrays marked by 1, 2, 3, 4, and 5. Each line array includes quadruplicated SPA spots and quadruplicated BSA spots. The red dashed line with arrows indicates the scanning path of the detection light spot OIRD.

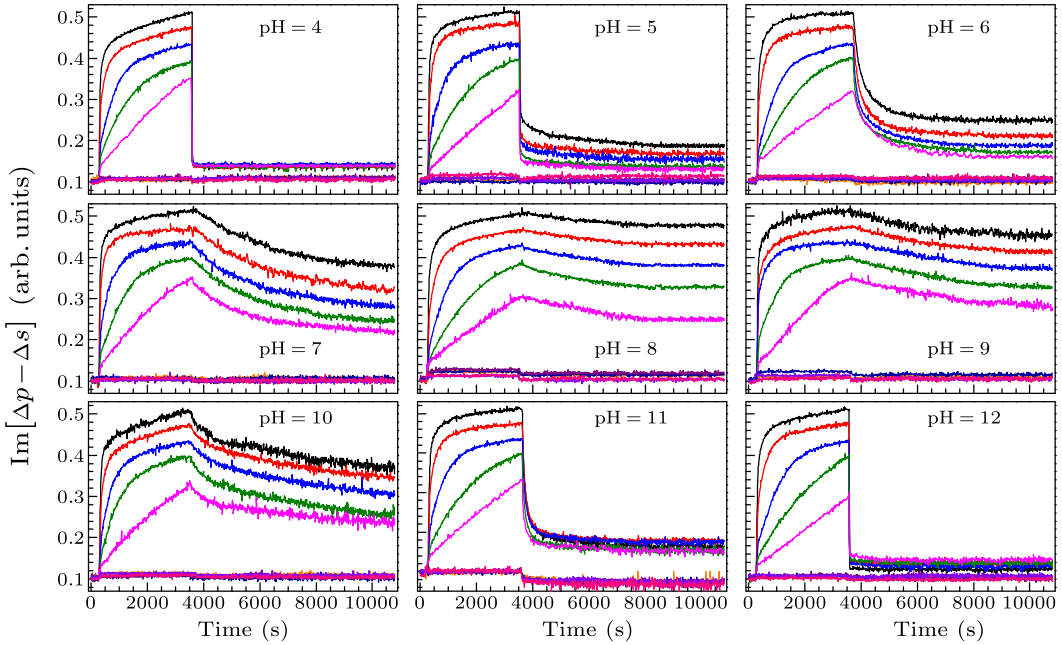

Fig. 2. The OIRD kinetic curves of binding between SPA and swine IgG at different concentrations and dissociations in a phosphate buffer with different pH values. The five lines showing an exponential behavior are obtained from SPA sample spots. Swine IgG concentrations corresponding to the five lines from top to bottom are 100 μg/mL, 50 μg/mL, 25 μg/mL, 12.5 μg/mL, and 6.25 μg/mL, respectively. The five lines closed to the baseline are obtained from BSA sample spots.

First, we monitored the binding processes between SPA and swine IgG (20831, KPL Inc. USA) at different concentrations by OIRD. The scanning program of the OIRD was carried out and the scanning light-spot moved repeatedly back and forth along the center line of the sample spots in the five line arrays (marked with the red dash line in Fig. 1). In this work, we collected the imaginary part signal of OIRD, $\mathrm{Im}\{\Delta_\mathrm{p} - \Delta_\mathrm{s}\}$. The baseline value of each spot was measured under the condition of the cavities filled with ddH_2O. Then,

the swine IgG solutions at five different concentrations 100, 50, 25, 12.5, and 6.25 μg/mL were pumped into the five cavities in parallel. The reaction and OIRD real-time monitor were sustained for 60 min.

After that, we monitored the dissociation processes of SPA-swine IgG complex in a phosphate buffer solution with different pH values. We selected nine pH values, 4, 5, 6, 7, 8, 9, 10, 11, and 12, and pumped the phosphate buffer into the five cavities with one of the same pH value every time after one of the SPA microarrays reacted with swine IgG. The phosphate buffers, pH=4, 5, 6, 7, 8, and 9, were obtained by mixing disodium hydrogen phosphate (Na_2HPO_4) solution and sodium citrate ($C_6H_5Na_3O_7{\cdot}2H_2O$) solution, and pH=10, 11, and 12 were obtained by mixing Na_2HPO_4 solution and sodium hydroxide (NaOH) solution. The dissociation and OIRD real-time monitor were sustained for 120 min.

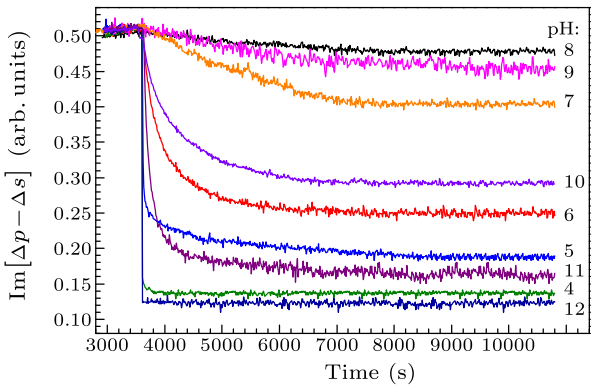

Fig. 3. The dissociation kinetic curves of SPA-swine IgG complex in the different pH values of phosphate buffer: pH=4, pH=5, pH=6, pH=7, pH=8, pH=9, pH=10, pH=11 and pH=12.

Figure 2 shows the nine kinetic curves of bindings and dissociations between SPA and swine IgG monitored by OIRD for the different pH values of phosphate buffer. Every value in the curves of Fig. 2 is the average value of OIRD $\mathrm{Im}\{\Delta_p - \Delta_s\}$ signals' intensities of the SPA or BSA quadruplicates in one cavity. The ON and OFF curves of the OIRD $\mathrm{Im}\{\Delta_p - \Delta_s\}$ signal intensities correspond to the dynamic processes of binding and dissociation of SPA and swine IgG, respectively. From Fig. 2, for the binding processes, it can be seen that the OIRD $\mathrm{Im}\{\Delta_p - \Delta_s\}$ intensities of BSA spots are horizontal, indicating that the BSA did not react with swine IgG, and all of the OIRD $\mathrm{Im}\{\Delta_p - \Delta_s\}$ signal intensities of SPA spots changed with the reaction time and showed an exponential behavior, meaning that the SPA reacted with swine IgG. The changes of $\mathrm{Im}\{\Delta_p - \Delta_s\}$ signal intensities for the various concentrations of swine IgG were different. The higher the swine IgG concentration was, the larger the $\mathrm{Im}\{\Delta_p - \Delta_s\}$ signal was, meaning that there was a faster binding velocity for the higher concentration of swine IgG. For the dissociation processes, the change tendencies of $\mathrm{Im}\{\Delta_p - \Delta_s\}$ signal intensities for the phosphate buffers with different pH values are tremendously different. In other words, the dissociation velocity of SPA-swine IgG complex is very different for the different pH values of the phosphate buffers. All of the bound swine IgG with the different concentrations was immediately dissociated when the pH value of phosphate buffer is 4 or 12, suggesting that the dissociation time almost does not correlate with the concentration of SPA and swine IgG. The dissociation velocity became slower and slower when the pH value of phosphate buffer gradually approaches 8 from 4 or 12. The dissociation velocities are almost constant for the bound swine IgG with different concentrations, i.e., only a certain percentage of the bound swine IgG could be dissociated, when the pH values of phosphate buffer are in the range of 5–11.

The effect of pH values of phosphate buffer on dissociation is further addressed by Fig. 3, which displays the dissociation kinetic curves in the phosphate buffer of nine different pH values for the complex of 1 mg/mL SPA and 100 μg/mL swine IgG. The dissociation curves in Fig. 3 for the different pH values of phosphate buffers have different dampings and equilibrium times. We can analyze the biochemistry interactions using the following equation[23]

$$I_t = (I_0 - I_\infty)e^{\frac{-(t-t_0)}{T}} + I_\infty, \tag{1}$$

where I_t is the OIRD signal at time t, t_0 is the moment where the dissociation beginning, I_0 is the OIRD signal at $t = t_0$, T is the dissociation time from t_0 to the equilibrium, and I_∞ is the extrapolated final OIRD signal. Thus $I_0 - I_\infty(\Delta I)$ is the damping coefficient.

Table 1. The relationship between among ΔI, T(s) and pH values

pH	ΔI	T(s)
4	0.384	5
5	0.251	84
6	0.253	458
7	0.158	1727
8	0.032	2287
9	0.071	1717
10	0.161	458
11	0.364	154
12	0.404	2

As shown in Fig. 3, although the OIRD signals in all nine curves eventually reach steady values, nearly none return to their baselines, suggesting that not all of the bound swine IgG can be dissociated in these situations. Therefore, the damping coefficient ΔI can be used to qualitatively denote the quantity or production of dissociated swine IgG. The damping coefficient ΔI and the dissociation time T(s) of the nine dissociation curves can be obtained by fitting the curves with Eq. (1). The fitting results of ΔI and T(s), as well as pH values, are list in Table 1. The damping coefficient ΔI corresponding to the pH value of 4 or

12 is about 12 times larger than that corresponding to the pH value of 8, while the dissociation time T(s) for the pH value of 8 is about 500 times larger than that for the pH value of 4 or 12, suggesting that choosing the appropriate pH value of phosphate buffer is very important to effectively purify swine IgG.

In summary, we have monitored the bindings between SPA and swine IgG with different concentrations as well as the dissociations of SPA-swine IgG complex in a phosphate buffer with different pH values by OIRD in a label-free and real-time fashion. The ON and OFF reaction dynamic curves corresponding to the bindings and dissociations have been obtained. The marked differences in damping coefficients and the dissociation times of SPA and swine IgG for nine pH values indicate that choosing an appropriate pH value of phosphate buffer is very important to effectively purify IgG. The results prove that the OIRD technique is a promising method for monitoring the dynamic processes of binding and dissociation of biomolecules.

References

[1] Zhu H, Bilgin M, Bangham R, Hall D, Casamayor A, Bertone P, Lan N, Jansen R, Bidlingmaier S, Houfek T, itchell T, Miller P, Dean R A, Gerstein M and Snyder M 2001 *Science* **293** 2101

[2] Espina V, Woodhouse E C, Wulfkuhle J, Asmussen H D, Petricoin E F and Liotta L A 2004 *J. Immunol. Methods* **290** 121

[3] Yu X B, Xu D K and Cheng Q 2006 *Proteomics* **6** 5493

[4] Ray S, Mehta G and Srivastava S 2010 *Proteomics* **10** 731

[5] Thiel A J, Frutos A G, Jordan C E, Corn R M and Smith L M 1997 *Anal. Chem.* **69** 4948

[6] Nelson B P, Frutos A G, Brockman J M and Corn R M 1999 *Anal. Chem.* **71** 3928

[7] Fei Y Y, Landry J P, Sun Y S, Zhu X D, Luo J T, Wang X B and Lam K S 2008 *Rev. Sci. Instrum.* **79** 013708

[8] He L P, Liu S, Dai J, Lu H B, Jin K J and Yang G Z 2014 *Sci. Chin. Phys. Mech. Astron.* **57** 615

[9] Wang X, Yuan K, Lu H, Wen J, Lu H B, Jin K J, Zhou Y L, Yang G Z, Li W and Ruan K C 2010 *J. Appl. Phys.* **107** 063109

[10] Wang J Y, Dai J, He L P, Sun Y, Lu H B, Jin K J and Yang G Z 2012 *J. Appl. Phys.* **112** 064702

[11] Sun Y, He L P, Dai J, Wang J Y, Lu H B, Wang S F, Jin K J, Zhou Y L and Yang G Z 2012 *Chin. Sci. Bull.* **57** 2898

[12] He L P, Dai J, Sun Y, Wang J Y, Lu H B, Wang S F, Jin K J, Zhou Y L and Yang G Z 2012 *Chin. Phys. Lett.* **29** 070702

[13] He L P, Sun Y, Dai J, Wang J Y, Lu H B, Wang S F, Jin K J, Zhou Y L and Yang G Z 2012 *Sci. Chin. Phys. Mech. Astron.* **55** 1585

[14] Wang X, Lu H, Dai J, Wen J, Yuan K, Lu H B, Jin K J, Zhou Y L and Yang G Z 2011 *Chin. Phys.* B **20** 010704

[15] Liu S, Zhu J H, He L P, Dai J, Lu H B, Wu L, Jin K J, Yang G Z and Zhu H 2014 *Appl. Phys. Lett.* **104** 163701

[16] Hu S H, Wan, J, Su Y J, Song Q F, Zeng Y X, Nguyen H N, Shin J H, Cox E, Rho H S, Woodard C, Xia S L, Liu S, Lyu H B, Ming G L, Wade H, Song H J, Qian J and Zhu H 2013 *eLife* **2** 00726

[17] Yuan K, Wang X, Lu H, Wen J, Lu H B, Zhou Y L, Jin K J, Yang G Z, Li W and Ruan K C 2010 *Sci. Chin. Phys. Mech. Astron.* **53** 143

[18] Lu H, Wen J, Wang X, Yuan K, Lu H B, Zhou Y L, Jin K J, Yang G Z, Li W and Ruan K C 2010 *Sci. Chin. Phys. Mech. Astron.* **53** 1230

[19] Lu H, Wen J, Wang X, Yuan K, Lu H B, Zhou Y L, Jin K J, Ruan K C and Yang G Z 2010 *J. Opt.* **12** 095301

[20] Dai J, Li L, Wang J Y, He L P, Lu H B, Ruan K C, Jin K J and Yang G Z 2012 *Sci. Chin. Phys. Mech. Astron.* **55** 2347

[21] Godfrey M, Kwasowski P, Clift R and Marks V 1993 *J. Immunol. Methods* **160** 97

[22] Moreno A I B, Bas C A, Rodríuez M, Conde I B B, Carballo S F and Martinez L 2003 *Hybrid Hybridomics* **22** 393

[23] Haake H M, Schütz A and Gauglitz G 2000 *Fresenius' J. Anal. Chem.* **366** 576